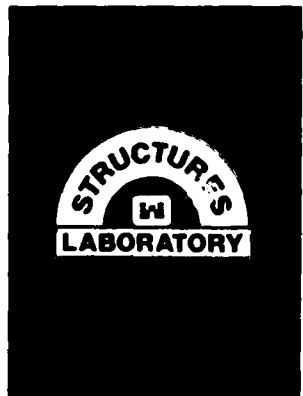
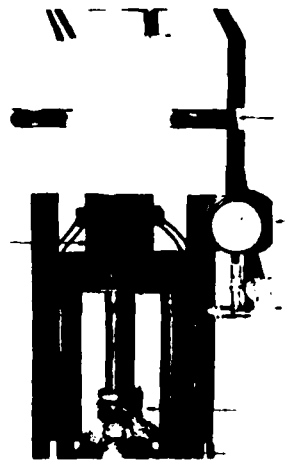
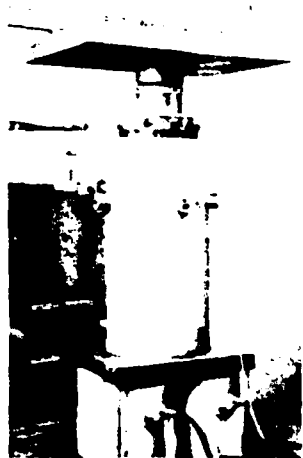


MICROCOPY RESOLUTION TEST CHART  
NATIONAL BUREAU OF STANDARDS-1963-A



US Army Corps  
of Engineers



AD-A160 444

MISCELLANEOUS PAPER SL-85-13

12

# CREEP TEST OF WIPP SITE ANHYDRITE CORE

by

Richard L. Stowe

Structures Laboratory

DEPARTMENT OF THE ARMY  
Waterways Experiment Station, Corps of Engineers  
PO Box 631, Vicksburg, Mississippi 39180-0631



September 1985  
Final Report

Approved For Public Release; Distribution Unlimited

DTIC FILE COPY

DTIC  
ELECTE  
OCT 22 1985  
S A D

Prepared for  
US Department of Energy  
Columbus, Ohio 43201

85 10 22 023

Destroy this report when no longer needed. Do not return  
it to the originator.

The findings in this report are not to be construed as an official  
Department of the Army position unless so designated  
by other authorized documents.

The contents of this report are not to be used for  
advertising, publication, or promotional purposes.  
Citation of trade names does not constitute an  
official endorsement or approval of the use of  
such commercial products.

Unclassified

SECURITY CLASSIFICATION OF THIS PAGE (When Data Entered)

REPORT DOCUMENTATION PAGE		READ INSTRUCTIONS BEFORE COMPLETING FORM
1. REPORT NUMBER Miscellaneous Paper SL-85-13	2. GOVT ACCESSION NO. AD-A160444	3. RECIPIENT'S CATALOG NUMBER
4. TITLE (and Subtitle)  CREEP TEST OF WIPP SITE ANHYDRITE CORE		5. TYPE OF REPORT & PERIOD COVERED Final report
7. AUTHOR(s)  Richard L. Stowe		6. PERFORMING ORG. REPORT NUMBER
9. PERFORMING ORGANIZATION NAME AND ADDRESS US Army Engineer Waterways Experiment Station Structures Laboratory PO Box 631, Vicksburg, Mississippi 39180-0631		8. CONTRACT OR GRANT NUMBER(s)  Contract No. DE-AI97-81ET 46633
11. CONTROLLING OFFICE NAME AND ADDRESS US Department of Energy Columbus, Ohio 43201		10. PROGRAM ELEMENT, PROJECT, TASK AREA & WORK UNIT NUMBERS
14. MONITORING AGENCY NAME & ADDRESS (if different from Controlling Office)		12. REPORT DATE September 1985
		13. NUMBER OF PAGES 28
		15. SECURITY CLASS. (of this report) Unclassified
		15a. DECLASSIFICATION/DOWNGRADING SCHEDULE
16. DISTRIBUTION STATEMENT (of this Report) Approved for public release; distribution unlimited.		
17. DISTRIBUTION STATEMENT (of the abstract entered in Block 20, if different from Report)		
18. SUPPLEMENTARY NOTES  Available from National Technical Information Service, 5285 Port Royal Road, Springfield, Virginia 22161.		
19. KEY WORDS (Continue on reverse side if necessary and identify by block number) Rock creep Anhydrite Waste Isolation Pilot Plant (WIPP). Repository sealing. —		
20. ABSTRACT (Continue on reverse side if necessary and identify by block number) —A creep reaction frame, a test specimen deformation jacket, a data acquisition system, and a triaxial chamber were readied and verified for their suitability for conducting triaxial creep tests of hard rock. All the equipment was found to be adequate for doint triaxial creep tests. A limited number of creep tests were conducted on anhydrite rock core from the Waste Isolation Pilot Plant (WIPP) site. Three of the four creep stages were observed during the testing. A logarithmic function was found to best fit the transient and steady-state creep stages.		

PREFACE

The work described in this report was done for the U. S. Department of Energy (DOE) under Contract DE-AI97-81ET46633 and modifications thereto. The original title of the project was "Investigation of Composition and Properties of Cementitious Mixtures for Boreholes and Shafts." This has now been changed to "Repository Sealing." Messrs. Floyd Burns, Lynn Myers and Don Moak of the Office of Nuclear Waste Isolation (ONWI) were earlier Project Managers. Mr. Steve Webster of the DOE-Columbus office is the current Project Manager.

This work was done in the Concrete Technology Division (CTD), Structures Laboratory (SL), of the U. S. Army Engineer Waterways Experiment Station (WES) under the direction of Mrs. Katharine Mather, Project Leader at that time. Mr. A. D. Buck is now the Project Leader. This specific work was done by Mr. R. L. Stowe, who prepared this report. Messrs. J. M. Scanlon and B. Mather were Chiefs of the CTD and SL, respectively.

Commander and Director of WES during the conduct of this study and the preparation of this report was COL Robert C. Lee, CE; Technical Director was Mr. F. R. Brown. During the publication of this report, COL Allen F. Grum, USA, was Director of WES; Dr. Robert W. Whalin was Technical Director.



Division For	
NTIS CRA&I	<input checked="" type="checkbox"/>
DTIC TAB	<input type="checkbox"/>
Unannounced	<input type="checkbox"/>
Justification	
By _____	
Distribution/	
Availability Codes	
Avail and/or	
Special	

AI

CONTENTS

	<u>Page</u>
PREFACE . . . . .	1
CONVERSION FACTORS, NON-SI TO SI (METRIC) UNITS OF MEASUREMENT . . . .	3
PART I: INTRODUCTION . . . . .	4
PART II: SAMPLES . . . . .	6
PART III: EXPERIMENTAL . . . . .	7
Deformation Jacket . . . . .	7
Triaxial Chamber . . . . .	9
Creep Loading Frame . . . . .	9
Data Acquisition System . . . . .	10
Grout Mold . . . . .	10
Test Matrix . . . . .	13
PART IV: RESULTS . . . . .	14
Creep Testing, Confining Pressure Zero . . . . .	14
Triaxial Creep Tests . . . . .	15
Petrographic Examination . . . . .	16
PART V: CONCLUSIONS AND RECOMMENDATIONS . . . . .	18
REFERENCES . . . . .	20
FIGURES 1-8	

CONVERSION FACTORS, NON-SI TO SI (METRIC)  
UNITS OF MEASUREMENT

Non-SI units of measurement used in this report can be converted to SI (metric) units as follows:

<u>Multiply</u>	<u>By</u>	<u>To Obtain</u>
Fahrenheit degrees	5/9	Celsius degrees or Kelvins*
feet	0.3048	metres
inches	25.4	millimetres
angstroms	0.1	nanometres
pounds (force) per square inch	0.006894757	megapascals
pounds (mass)	0.45359237	kilograms
pounds (force)	4.448222	newtons
tons (force)	0.008896444	meganewtons

\* To obtain Celsius (C) temperature readings from Fahrenheit (F) readings, use the following formula:  $C = (5/9)(F - 32)$ . To obtain Kelvin (K) readings, use:  $K = (5/9)(F - 32) + 273.15$ .



## CREEP TEST OF WIPP SITE ANHYDRITE CORE

### PART I: INTRODUCTION

1. Rock salt from the Waste Isolation Pilot Plant (WIPP) site in southeastern New Mexico has been tested and analyzed extensively, the major purpose being in support of the structural design of the WIPP facilities. Researchers of the Sandia National Laboratories in Albuquerque, New Mexico, and at RE/SPEC in Rapid City, South Dakota, are responsible for the major testing effort. This work has been focused on the effect of stress and temperature on strength and deformation of the bedded rock salt; triaxial quasistatic compression and creep tests have been conducted (Hansen 1977 and 1979 and Wawersik 1979 and 1980).

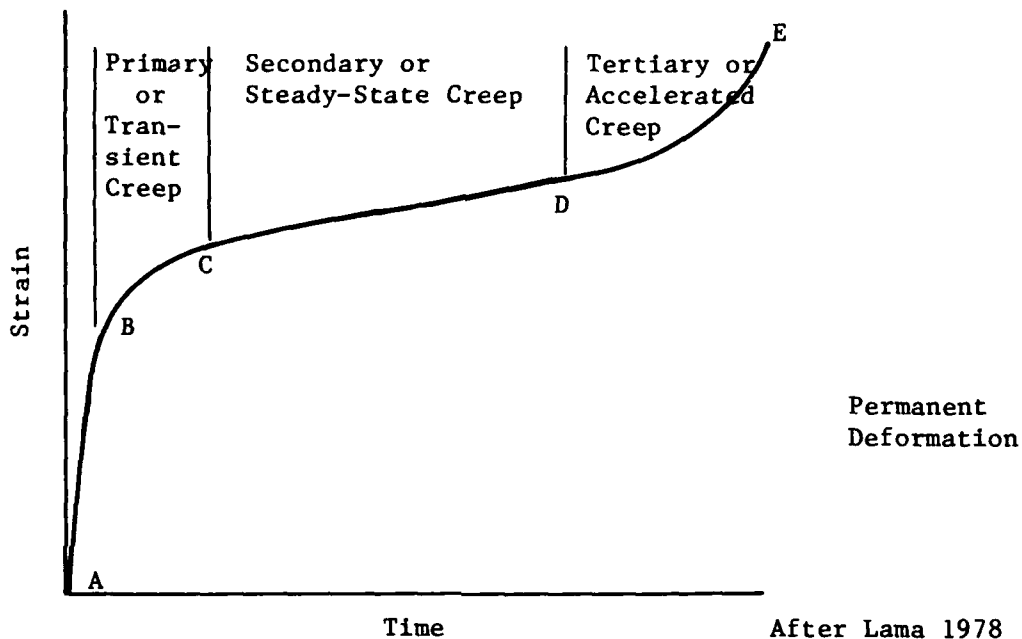
2. The various openings and plugs associated with the site will pass through or be contained within anhydrite and polyhalite stringers in the massive salt beds. Some quasistatic triaxial compression tests have been conducted on cores recovered from these stringers (Pfeifle 1980). Little effort has been directed towards understanding the creep behavior of the anhydrite or the polyhalite. To our knowledge candidate cementitious grouts, to be used in plugs, have not been tested for the effect of stress and temperature on strength and deformation.

3. The objective of this investigation was to determine the uniaxial compressive strength and triaxial creep characteristics of anhydrite. Three anhydrite cores were tested in creep. It was proposed to do extensive creep testing on the candidate grout designated BCT-1 FF (Gulick 1980). However creep testing of the grout was not done due to the time it took to ready and verify the triaxial chamber, the creep rig, and the deformation jacket to monitor specimen deformations.

4. This report describes the equipment used to test the anhydrite core in triaxial creep; test results from the core are presented. Information is presented on preliminary work to ascertain a suitable technique for making grout specimens for creep testing. A test matrix is proposed for further anhydrite and grout testing. The following information is presented as a review of some

of the terms used in creep testing. An idealized creep curve for rock subjected to a constant stress is given below. The curve shows the separation into four stages for analytical convenience. Lama's (1978) definitions are used:

1. The instantaneous elastic strain (AB),
2. primary or transient creep (BC),
3. secondary or steady-state creep (CD) and
4. tertiary or accelerated creep (DE).



"The instantaneous elastic strain (AB) occurs immediately on application of load and is followed by primary creep in which the rate of strain decreases with time.

"If the stress is allowed to persist beyond (C), secondary creep sets in where the strain-rate is constant and the specimen undergoes permanent deformation. If specimen is destressed at any point between the range (CD), the permanent deformation takes place. The amount of permanent deformation is governed by steady strain rate  $\dot{\epsilon}$  and the time elapsed.

"If the specimen is not destressed at the point (D), the rate of strain increases at an increasing rate and the specimen eventually fails. This phase (DE) is called tertiary creep. This creep phase, if once initiated, is usually so short that failure cannot be arrested. The tertiary creep does not represent a pure deformation process but progressive damage and is fundamentally different from the two preceding stages of deformation. All the three stages of creep are observed only at proportionally high stress levels."

## PART II: SAMPLES

5. Two short pieces of 4-in.\*-diameter rock core from Hole AEC-7 at the WIPP site in New Mexico were selected for creep testing. The rock was supposed to be anhydrite, a brief petrographic examination was made to check this supposition.

6. Each piece of core was about 4 in. long; they were identified as 4344 and -4344. This identification meant they were from a depth of about 4344 ft. Since the placement of Plugs 1 and 2 in AEC-7 during the Bell Canyon Test were at a depth of about 4500 ft and this anhydrite formation is approximately 400 ft thick in this region, these samples are the same anhydrite formation that contacts Plugs 1 and 2 (Christensen and Peterson (1981)).

7. The 4-in. cores were set in shallow boxes, concreted in place, and redrilled using a NX size core barrel. The redrilled core diameter was 2.125 in. The pieces were prepared for testing using the Corps of Engineers Rock Testing Handbook (RTH) methods RTH 103-80 and RTH 111-80, (U. S. Army Engineer Waterways Experiment Station (WES) 1980). The two cores are designated AC No. 1 and AC No. 2.\*\*

8. A candidate grout (BCT-1FF) was mixed and placed in a closed-ended cylinder. The cylinder was used in an attempt to find a suitable mold for casting grout creep test specimens. As indicated earlier, this effort terminated after development of the mold.

---

\* A table of factors for converting non-SI to SI (metric) units of measurement is presented on page 3.

\*\* A stands for anhydrite, C for creep test, and No. 1 and No. 2 for number of core.

## PART III: EXPERIMENTAL

### Deformation Jacket

9. The strain measuring apparatus used to obtain creep strain on the anhydrite core was a SBEL,<sup>(1)</sup> DJC Deformation Jacket,<sup>(2)</sup> (Figure 1). The jacket is designed for longitudinal and lateral strain measurements on NX-size rock cores. Three linear variable differential transducers (LVDT) are spaced 120 degrees apart on each axis. The LVDT's are capable of monitoring up to 1/4-in. movements. The device is attached to the specimen with small screws.

10. The top and bottom rings have three gauge points each that are screwed into the specimen with light hand pressure. The gauge points are positioned in the longitudinal axis so that a gauge factor of 2.50 in. is obtained. Because gauges relying on friction contact are not permissible (RTH 205-80) (WES 1980) in creep testing, small, shallow holes were drilled into the test specimen. The gauge points were recessed into the specimen about 1/64 in. The middle ring contains the three horizontal LVDT's and is not attached to the specimen; it is supported on spring-loaded rods that are attached to the lower ring.

11. The deformation characteristics of a device similar to the SBEL unit was reported by Hardy (1970). He found that for two rocks, aluminum, brass, and steel cylinders, the clamp-on strain transducers gave similar Young's modulus and Poisson's ratio, as did bonded resistance-type strain gauges. Young's modulus differed by less than 2 percent and Poisson's ratio by less than 3 percent for all materials tested. In view of Hardy's results, a limited evaluation program of the SBEL jacket was conducted.

12. An aluminum-bronze cylinder and two anhydrite cores have been used to date to evaluate the SBEL jacket. Testing details are presented in the following tabulation:

<u>Material</u>	<u>Strain Measuring Method</u>	<u>Load Application by</u>
Aluminum-bronze cylinder	Strain gauges Deformation jacket	440,000-lbf machine
Anhydrite, 4317 ft	Strain gauges	Creep loading frame
Anhydrite, 4344 ft	Strain gauges Deformation jacket	440,000-lbf machine Creep loading frame

(1) SBEL, Structures Behavior Engineering Laboratory.

(2) DJC is a series designation.

13. The aluminum cylinder was previously used in the laboratory as a load cell. Two SR-4 type strain gauges were bonded to the cylinder at midheight and parallel to the longitudinal axis. The length to diameter ratio (L/D) is 1.75 in. The material designation is not known. It is assumed to be either cast or wrought aluminum bronze with an ultimate strength in tension from 55,000 to 151,000 psi, a minimum yield strength of 20,000 psi, and a modulus of elasticity (E) from 15 to  $19 \times 10^6$  psi. The cylinder was used for a preliminary evaluation because it had machined ends and was strain gauged.

14. The cylinder was loaded in uniaxial compression in a 440,000-lb universal testing machine to an axial stress of 18,820 psi, strain readings being recorded during loading. Upon unloading, the deformation jacket was attached to the cylinder and the cylinder loaded as before. The results of these tests are presented in Figure 2.

15. A modulus of elasticity was computed as a tangent value from zero to the maximum applied stress. The values of Young's modulus obtained by the two methods differ by a maximum of 31 percent to a minimum of 20 percent. The comparison is considered unacceptable. This large deviation may be due to end effects and the relatively small axial strains involved. With a 2.5-in. gauge factor and a cylinder length of 3.68 in., it is likely that high confining stresses, causing end effects, would exist in the cylinder. The confining stresses are due to the difference in the modulus and Poisson's ratio of the aluminum cylinder and the steel platen of the testing machine. A new aluminum cylinder was made. It was designed so that end effects do not influence the deformation jacket measurements.

16. Only two short pieces of anhydrite core were available at the Waterways Experiment Station (WES) for creep testing. Due to the scarcity of core, it was thought that a comparison between measurements made with bonded strain gauges and the deformation jacket should be made. Strain gauge data obtained from a previously tested core (elevation 4317 ft) would be compared to the initial strain data from the first creep test, creep strain being measured with the deformation jacket. If an acceptable comparison resulted, then the creep test would be continued. Figure 3 illustrates the axial stress and axial strain data from the anhydrite obtained using bonded strain gauges and the deformation jacket.

17. Figure 3 presents the Young's moduli computed as tangent values for both cores. The modulus was taken at one-half the ultimate stress for specimen

4317 ft and at the same stress level for specimen 4344 ft. The moduli differed by 6 percent. This difference is acceptable considering that two different pieces of core and two different loading devices were used. Prior to additional creep tests, the new aluminum cylinder and a homogeneous rock will be used to further evaluate the SBEL<sup>(1)</sup> deformation jacket. At the present, the jacket is considered an acceptable device for measuring creep strains.

#### Triaxial Chamber

18. The triaxial chamber used in conducting triaxial creep tests is a SBEL Model 10 cell capable of lateral confining pressures ( $\sigma_2 = \sigma_3$ ) to 10,000 psi. Axial load capability is 300,000 lbf. The cell accepts NX size cores and the deformation jacket shown in Figure 1. Figure 1 shows the base of the cell including some of the electrical feed-through connectors for passage of strain gauge and deformation jacket electronic signals to external readout-recorder devices. The cell was designed to withstand temperatures to 200° C. The cell is presently not equipped for elevated temperature testing; however, external band heaters can be added without difficulty.

#### Creep Loading Frame

19. The loading frame used to conduct the creep test is illustrated in Figure 4. It consists of top and bottom header plates, midheader plates that constrained four railroad car springs acting as a load-maintaining element, a 60-ton force hydraulic ram used to apply a desired compression load, a 50,000-lbf load cell, and threaded rods to take the reaction of the loaded system. Load was maintained to within 2 percent of the total applied load using a hydraulic hand pump connected to the ram. The load was monitored with a digital multimeter that was connected to the load cell. Load was applied to the test specimen using the triaxial piston which is spherically seated into an end platen resting atop the specimen.

20. The 60-ton ram was calibrated using a hydraulic hand-operated pump and the 440,000-lb universal test machine. Pump pressure was monitored with a bourdon tube pressure gauge attached to the pump. Prior to the calibration of the ram, the pressure gauge was calibrated using a dead weight tester. The load cell was calibrated using the universal testing machine and a digital multimeter.

21. To verify that the creep loading system was functioning properly, the aluminum-bronze cylinder, previously mentioned, was loaded to a stress level of 18,820 psi. Strain gauge readings were made and the stress-strain data used to compute a Young's modulus. There was no difference in the modulus of the cylinder when loaded in the 440,000-lbf universal testing machine and the creep loading frame; the modulus is  $17.7 \times 10^6$  psi. The creep loading system is giving anticipated loads.

#### Data Acquisition System

22. Data collected during the creep test are axial stress, temperature, time, and axial and lateral strain. A Model 9300 Monitor Labs general-purpose data logger (Microprocessor control) was used to record the data. Output from signal conditioners were fed into the microprocessor which was programmed to output the data in selected engineering units. The stress, strain, and time data are analyzed using the WES Honeywell DPS1 computer. A Tektronix 4014-1 graphics terminal and Tektronix 4631 hard copy unit are interfaced with the computer and are used to input and receive data. The data acquisition system will shortly be upgraded with a data cassette interfaced with the 9300 logger. The cassette tape is then used with a Silent 700 electronic data terminal for data input to the computer.

#### Grout Mold

23. The BCT-1 FF grout contains about 1900 lb cement per cubic yard. The grout will expand due to the temperature rise resulting from the heat of hydration. To minimize the expansion and possible cracking it was decided to case the grout in a closed ended steel mold, allow the grout to expand to a near equilibrium state, saw off the steel mold, and test the grout under creep loads. During creep testing, a companion specimen will be monitored for any possible expansion. If additional expansion occurs in the control specimen, then the same amount of expansion will be subtracted from the grout specimen under test.

24. Strain gauges were used to monitor the expansion of the grout to a near equilibrium state. Two strain gauges were bonded to the outside of a 2-in. ID piece of seamless steel pipe; the pipe was "schedule 80" and 5 in. in

length; wall thickness was 0.2 in. The gauges were located at the cylinder midheight and positioned in the horizontal plane.

25. The cylinder had a hydraulic fitting through one of the closed ends, a piece of flat plate was welded to the ends. The cylinder was pressure tested using hydraulic fluid, cleaned, and then filled with the BCT-1 FF grout. The cylinder was calibrated by pressurizing it with hydraulic fluid to an internal pressure ( $p_i$ ) of about 700 psi. Strain measurements were made. The value of 700-psi internal pressure was selected because it was thought that the grout, once placed inside the cylinder, would produce a pressure against the cylinder side walls somewhat less than 700 psi. Three calibration runs were made. The calibration was made to see if the strain gauges could monitor the internal pressure due to the hydraulic fluid. If so, when the grout was placed inside the cylinder, the pressure produced by the grout could be ascertained. At the same time, the strain gauges would indicate when the grout expansion reached a near equilibrium state.

26. A plot of internal pressure versus the tangential or hoop strain ( $\epsilon_\theta$ ) is presented in Figure 5. Theoretical hoop strain calculations were made using Equation 1.

$$\epsilon_\theta = \frac{1}{E}(\tau_{\theta\theta} - \nu\tau_{rr}) \quad (1)$$

where  $\epsilon_\theta$  = theoretical hoop strain

E = Young's modulus of elasticity

$\tau_{\theta\theta}$  = hoop stress

$\nu$  = Poisson's ratio

$\tau_{rr}$  = radial stress

Young's modulus was assumed as  $29 \times 10^6$  psi and Poisson's ratio was assumed as 0.30.

27. The hoop stress was calculated using Equation 2.

$$\tau_{\theta\theta} = p_i \frac{r_i^2}{r_o^2 - r_i^2} \left( \frac{r_o^2}{r^2} + 1 \right) \quad (2)$$

where  $p_i$  = internal pressure

$r_i$  = inside radius

$r_o$  = outside radius

r = any radius



The radial stress in Equation (1) is equal to zero for the calculations of hoop stress at the outside surface of the cylinder. The theoretical pressure versus hoop strain is plotted in Figure 5.

28. As noted in Figure 5, the measured and theoretical hoop strains are divergent. A partial explanation for the difference is that the modulus and the physical measurements of the cylinder radii are somewhat in error. Heating up of the cylinder when the ends were welded on could have caused parts of the steel to have a different modulus than the assumed  $29 \times 10^6$  psi. The difference in the two curves is considered acceptable for the intended purpose.

29. The results of the strain gauged cylinder mold are presented in Figure 6. The strain gauges indicated an inward movement of 17 microinches (compressive force) of the cylinder mold at about 12 hr after casting. It is difficult to explain a compressive force existing in the cylinder wall. An inward movement of the cylinder wall would occur if the length of the cylinder increased. What would cause that to happen is not postulated.

30. At about 12 hr the strain gauges indicated an expansion of the cylinder wall. From day 1/2 to 2 days, a rather sharp increase in the hoop strain occurred, at which point the rate of strain began to decrease. At about 15 days the rate of strain decreased markedly. The hoop strain appears to approach a near constant rate at about 40 days. When grout specimens are made for creep testing, they will be allowed to cure in the steel molds for 40 to 50 days.

31. The maximum hoop strain recorded was 105 microinches. Figure 5 can be used to determine the internal pressure exerted on the 0.2-in.-thick cylinder wall by the expanding grout. At 105 microinches of hoop strain, the internal pressure is 850 psi.

32. The steel cylinder mold was cut open and the grout cylinder examined. First the ends were sawed off. Macroscopic examination of the ends indicated that the grout was not cracked. The steel cylinder was cut longitudinally, the grout removed and examined. The ends and sides of the grout were wiped clean and wetted with water. No macroscopic cracks were observed. Several days later a portion of the core, that was not tested in compression, was re-examined. The ends showed faint hairline cracks in an irregular pattern. The cracks probably occurred due to stress relieving. This phenomenon has been observed before in restrained and unrestrained grout samples made with similar quantities of cement. The apparent specific gravity of the grout is 2.11 g/cc and the compressive strength at 133-day age is 13,210 psi.

Test Matrix

33. Three anhydrite cores were tested in triaxial creep with the confining pressure equal to zero and 1000 psi and at a temperature of 24° C. One specimen tested at zero confining pressure was unsaturated while the other two specimens were saturated. The creep test matrix is presented in the following tabulation for the anhydrite.

Test Matrix for Anhydrite

	T = 24° C		
	Unsaturated	Saturated	
$\sigma_1 - \sigma_2$ — $\sigma_2 = \sigma_3$	0	0	1000
13,200 for $\sigma_2 = 0$			
12,200 for $\sigma_2 = 1000$	1		1
17,620		1	

Stress units are psi; entries indicate number of tests to be run.  $\sigma_1$ ,  $\sigma_2$ ,  $\sigma_3$  are the principal stresses.

## PART IV: RESULTS

### Creep Testing, Confining Pressure Zero

34. The results of the creep test of anhydrite cores No. AC-1 and AC-2<sup>(3)</sup> are presented in Figure 7; the axial strain is presented as a function of time. Axial stress difference load rates were applied rapidly so that creep strain did not occur, or was minimized, before the after-loading strain was observed. The specimens were tested for a total of 50.5 days at a constant load of 13,200 psi and 17,620 psi. These constant loads are equal to a ratio of applied principal stress difference  $(\sigma_1 - \sigma_2)$ <sup>(4)</sup> to compressive strength ( $q_u$ ),  $\sigma_1 - \sigma_2/q_u$  equal to 0.6 and 0.8, respectively. The estimated  $q_u$  of the anhydrite is 22,020 psi. This is an average value obtained from previous testing of anhydrite cores from about 30-ft distance from the location of Specimens AC-1 and AC-2.

35. The creep curves in Figure 7 have three distinct stages; an instantaneous elastic strain stage, a transient creep stage, and a steady-state creep stage. The elastic strain for Specimen AC-1 lies between zero and 977 micro-inches which occurred in the first 16 minutes of loading to the required constant load. For Specimen AC-2 the elastic strain stage extends to 1692 micro-inches which was reached in about 60 minutes of loading to  $0.8 q_u$ . Almost all the elastic strain was recovered upon unloading the specimens at 50.5 days; this would be expected for a sound rock that had not undergone much permanent deformation. The transient creep stage for the specimen loaded to  $0.6 q_u$  and  $0.8 q_u$  lasted for 16.5 and 29 days, respectively. The steady-state stage for both specimens continued to termination of the test. Tertiary creep was not observed, it would be expected to occur at higher  $\sigma_1 - \sigma_2/q_u$  ratios or at longer test times. The transition between transient and steady-state creep was ascertained by drawing a straight line tangent to the curve in the steady-state region. The beginning of the steady-state creep is where the transient creep curve touches this straight line.

36. Previous investigators have used power curve fits, exponential curve fits, and logarithmic curve fits to describe creep in metals and geologic materials. Griggs (1939) used a logarithmic law to describe the "elastio-viscous flow" in several rocks. Some researchers have used one law to fit the

---

(3) AC = anhydrite creep sample No. 1.

(4)  $\sigma_1$  = maximum principal stress;  $\sigma_2$  = minimum principal stress.

transient creep and another law to fit the steady-state creep. It appears that no one acceptable method of describing creep of rocks exists. The anhydrite creep data were found to fit best when a logarithmic function was used. The following equation fits well for both the transient and steady-state stages for Specimens AC-1 and AC-2.

Specimen

$$\text{AC-1} \quad \epsilon = 1024.08 + 16.97 \ln t \quad (3)$$

$$\text{AC-2} \quad \epsilon = 1743.65 + 28.21 \ln t \quad (4)$$

where  $\epsilon$  is the creep strain, and  $t$  is time

The correlation coefficient ( $r^2$ ) for Equation 3 is 0.97, and for Equation 4 it is 0.87. Attempts were made to fit the transient and steady-state creep observed on both specimens with a power function and exponential function; however, neither fit as well as the logarithmic function.

37. The strain rate ( $\dot{\epsilon}$ ) for the steady-state creep was obtained by computing the slope of strain time curves. The strain rate is  $6.2 \times 10^{-12}$   $\mu\text{in.}/\text{in. s}^{-1}$  for Specimen AC-1 and  $2.64 \times 10^{-11}$   $\mu\text{in.}/\text{in. s}^{-1}$  for Specimen AC-2. The relatively faster strain rate exhibited by Specimen AC-2 is expected due to the higher axial load applied to this specimen.

Triaxial Creep Tests

38. One triaxial creep test was conducted at a temperature of  $24^{\circ}$  C, a confining pressure of 1000 psi, and stress difference of 12,200 psi. The ratio of  $(\sigma_1 - \sigma_2)/q_u$  was 0.55. The specimen was tested for a total of 79.5 days. This part of the report presents and discusses axial deformation data within the transient and the steady-state stages for Specimen AC-3. The results of the creep test of Specimen AC-3 are presented in Figure 8; the axial strain is presented as a function of time.

39. The creep curve in Figure 8 exhibits inelastic, transient, and steady-state creep. The transient creep stage, i.e., that region where the strain rate continuously decreases, lasted for 57.5 days. Steady-state creep continued until the test was terminated. No tertiary creep was observed. Tertiary creep would be expected at high ratios of  $\sigma_1 - \sigma_2/q_u$  and higher confining pressures for a sound rock like the anhydrite tested in this study.

40. The triaxial creep data were found to fit best when a logarithmic function was used. The following equation was obtained for both the transient and steady-state stages.

$$\epsilon = 1224.95 + 17.73 \ln t \quad (5)$$

The equation fits the data fairly well, as indicated by the correlation coefficient of 0.86. Attempts were made to fit the transient and the steady-state creep regions with a power function and an exponential function; however, neither fitted as well as the logarithmic function.

41. The strain rate for the steady-state creep stage is  $4.82 \times 10^{-12}$   $\mu\text{in./in. s}^{-1}$  for Specimen AC-3 and was obtained using linear regression. This strain rate is slightly less than the strain rate obtained on Specimen AC-1 ( $6.2 \times 10^{-12}$   $\text{s}^{-1}$ ) which was tested at about the same ratio of  $\sigma_1 - \sigma_2/q_u$  but without confining pressure. Robertson's (1960) experiments permit the important conclusion that hydrostatic pressure greatly decreases the transient creep rate of Solenhofen limestone when tested in a state of triaxial confinement. The decrease in steady-state creep rates could be expected as well. The strain rates observed in this study for the steady-state region of creep indicate that confining pressure has decreased the creep rate somewhat for the anhydrite. Additional testing of the anhydrite should be done to verify any change in creep rate in the transient and steady-state stages with increased differential stress, confining pressure, and temperature. The creep rate of any host rock in and around a repository is an important design consideration.

#### Petrographic Examination

42. The X-ray data showed that neither piece of core was pure anhydrite; each contained substantial amounts of carbonate minerals and some quartz. The composition and relative amounts of each mineral in the samples are shown below:

Constituents	Relative Amounts <sup>(a)</sup> in Samples from Depths, Ft	
	4344	-4344
Anhydrite	A	I
Dolomite	C	I
Calcite	C	I
Quartz	R	R <sup>(b)</sup>
Magnesite	Not detected	R

(a) Relative amounts were estimated by peak intensity and were indicated as follows: Abundant (A) = >50 percent, Intermediate (I) = 25 to 50 percent, Common (C) = 10 to 25 percent, Rare (R) = <5 percent.

(b) Tentatively identified by a single XRD peak.

43. Several scraps of core and one piece of core 2.7 ft long from this hole representing a depth of about 4500 ft were examined and reported earlier (Gulick et al 1980 and Christenson and Peterson 1981). Those samples were anhydrite rock with some dolomite and less quartz and plagioclase feldspar. The present samples came from about 150 ft higher in the formation than the earlier samples. Both sets were impure anhydrite with the present samples being considerably more impure.

## PART V: CONCLUSIONS AND RECOMMENDATIONS

44. The major portion of this study was gearing up and verifying suitability of equipment for triaxial creep testing. The limited amount of testing, due basically to the lack of suitable anhydrite core on hand, has shown that the deformation jacket, creep loading frame, and triaxial chamber were suitable for creep testing of hard rock. For the test parameters used, the creep strain results appear reasonable for a strong tough rock like the anhydrite.

45. The anhydrite exhibited transient and steady-state creep. The axial strain versus time data fit well a logarithmic function which provides a limited assessment of the strain. The creep strains obtained cannot be considered as representative due to the limited testing; therefore, they are not compared with other creep strain data obtained by other investigators that have tested rock from the WIPP site.

46. The steady-state strain rates ranging from  $2.64 \times 10^{-11}$   $\mu\text{in./in. s}^{-1}$  to  $6.2 \times 10^{-12}$   $\mu\text{in./in. s}^{-1}$  are considered reasonable for the anhydrite. Indications are that the strain rate decreases with increased confining pressure. For those specimens tested without confining pressures, the steady-state strain rate increases with increased axial load.

47. It is recommended that triaxial creep testing on the anhydrite be continued to include temperatures to  $100^{\circ}\text{C}$ , axial stress differences to 50 percent of the average unconfined compressive strength of the rock, and confining pressures of about 6000 psi.

48. It is recommended that triaxial creep testing be initiated on selected grout. To our knowledge, no creep data exist on the types of grouts that would likely be used for repository sealing. Creep test experimental limits for grout are recommended as follows:

Temperature:  $24 \leq \text{Specimen} \leq 100 \text{ C}$

Axial Stress Difference:  $3,000 \leq \sigma_1 - \sigma_2 \leq 11,000 \text{ psi}$

Confining Pressures:  $1,000 \leq \sigma_2 = \sigma_3 \leq 6,000 \text{ psi}$

As a starting recommendation for creep testing of the grout, the following tabulation is offered.

Matrix of Tests for BCT-1-FF Grout

$\sigma_1 - \sigma_2$ / $\sigma_2 = \sigma_3$	T = 24° C				T = 100° C			
	1000	2000	4000	6000	1000	2000	4000	6000
3,000	3	3	3	3	3	3	3	3
6,000			3				3	
9,000			3				3	
11,000	3		3				3	

Stress units are psi. Entries indicate number of tests to be run.

49. Examination of two samples of core from a depth of about 4344 ft in Hole AEC-7 showed them to be impure anhydrite.

50. Comparison with earlier samples from approximately 150 ft deeper showed general similarity with the present samples being more impure.



## REFERENCES

- Christensen, C. L., and Peterson, E. W. 1981. "The Bell Canyon Test Summary Report," SAND 80-1375, Sandia National Laboratories, Albuquerque, NM.
- Griggs, D. 1939. "Creep of Rocks," J. Geol., Vol 47, No. 3, Apr-May, pp 225-251.
- Gulick, C. W., Jr.; Boa, J. A., Jr.; and Buck, A. D. 1980. "Bell Canyon Test (BCT) Cement Grout Development Report," SAND 80-1928, Sandia National Laboratories, Albuquerque, NM.
- Hansen, Francis D. 1977. "Triaxial Quasi-Static Compression and Creep Behavior of Bedded Salt from Southeastern New Mexico," RE/SPEC Inc., Rapid City, SD, RSI-0055, Sandia Laboratories, Albuquerque, NM, SAND 79-7045.
- Hansen, Francis D., and Mellegard, Kirby D. 1977. "Creep Behavior of Bedded Salt from Southeastern New Mexico at Elevated Temperature," RE/SPEC Inc., Rapid City, SD, RSI-0062, Sandia Laboratories, Albuquerque, NM, SAND 79-7030.
- Hansen, Francis D., and Mellegard, Kirby D. 1979. "Further Creep Behavior of Bedded Salt from Southeastern New Mexico at Elevated Temperature," RE/SPEC Inc., Rapid City, SD, RSI-0104, Sandia Laboratories, Albuquerque, NM, SAND 80-7114.
- Hardy, H. Reginald, Jr.; and Kim, Y. S. 1970. "A Clamp-On Strain Transducer for Use on Geologic Materials," Reprinted from Society of Petroleum Engineers Journal, Mar 1970.
- Lama, R. D., and Vutukuri, V. S. 1978. "Handbook on Mechanical Properties of Rocks - Testing Techniques and Results," Vol III, Trans Tech Publications, Herzberg, Germany, p 237.
- Pfeifle, Tom W., and Senseny, Paul E. 1980. "Elastic-Plastic Deformation of Anhydrite and Polyhalite as Determined from Quasi-Static Triaxial Compression Tests," RE/SPEC Inc., Rapid City, SD, RSI-0135, Sandia Laboratories, Albuquerque, NM, SAND-81-7063.
- Robertson, E. C. 1960. "Creep of Solenhofen Limestone Under Moderate Hydrostatic Pressure," Geol. Soc. Am. Mem. 79, pp 227-244.
- U. S. Army Engineer Waterways Experiment Station, CE. 1980. "Rock Testing Handbook," Test Standards - 1980, Vicksburg, MS.
- Wawersik, Wolfgang R., and Hannum, David W. 1979. "Mechanical Behavior of New Mexico Rock Salt in Triaxial Compression Up to 200° C," Sandia Laboratories, Albuquerque, NM, SAND 77-1192.
- Wawersik, Wolfgang R., and Hannum, David W. 1980. "Interim Summary of Sandia Creep Experiments on Rock Salt from the WIPP Study Area, Southeastern New Mexico," Sandia Laboratories, Albuquerque, NM, SAND 79-0115.

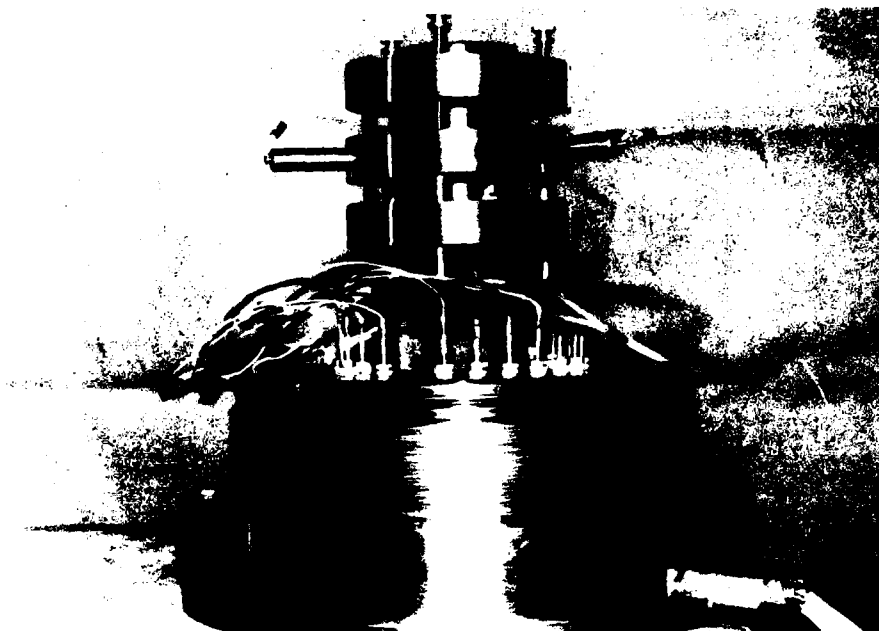


Figure 1. Deformation device shown attached to blank specimen that is resting on the triaxial chamber base platen

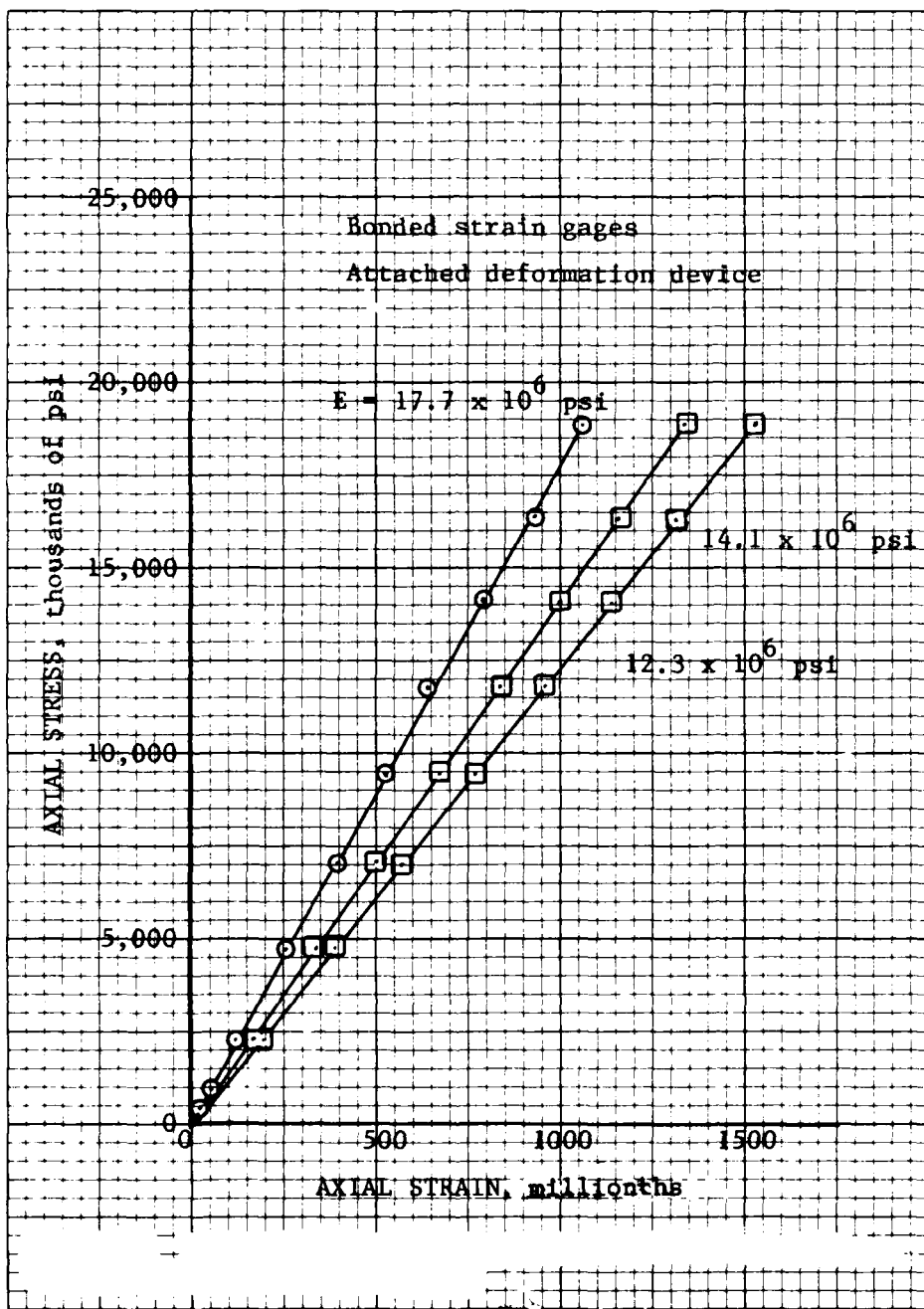


Figure 2. Axial stress versus axial strain for aluminum bronze cylinder  
 obtained using bonded strain gauges and deformation device,  
 440,000-lbf universal testing machine

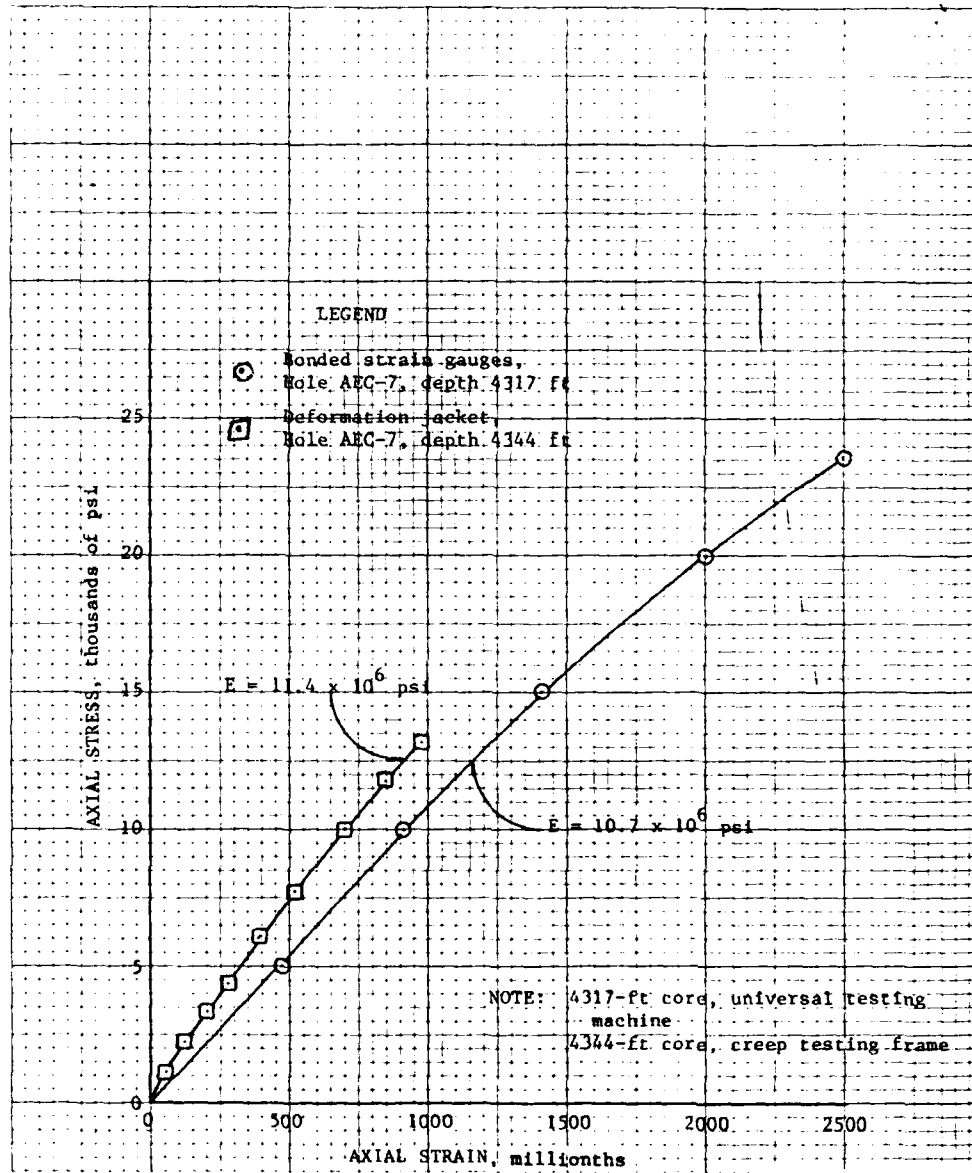


Figure 3. Axial stress versus axial strain for anhydrite cores obtained using bonded strain gauges and deformation jacket

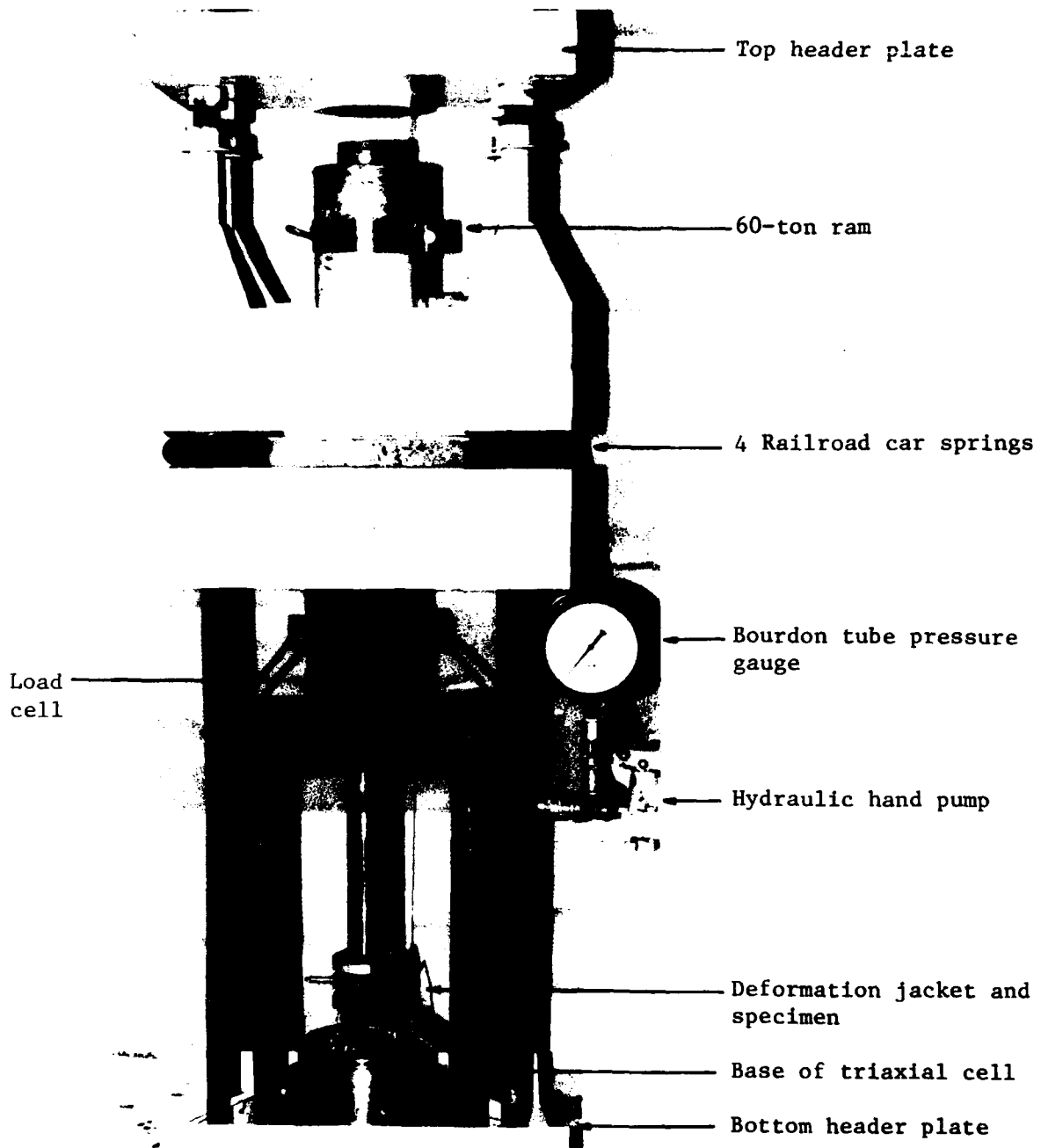


Figure 4. Creep loading frame; springs used to maintain axial load. Triaxial base platen with deformation jacket, specimen and loading piston in place; chamber portion not in place

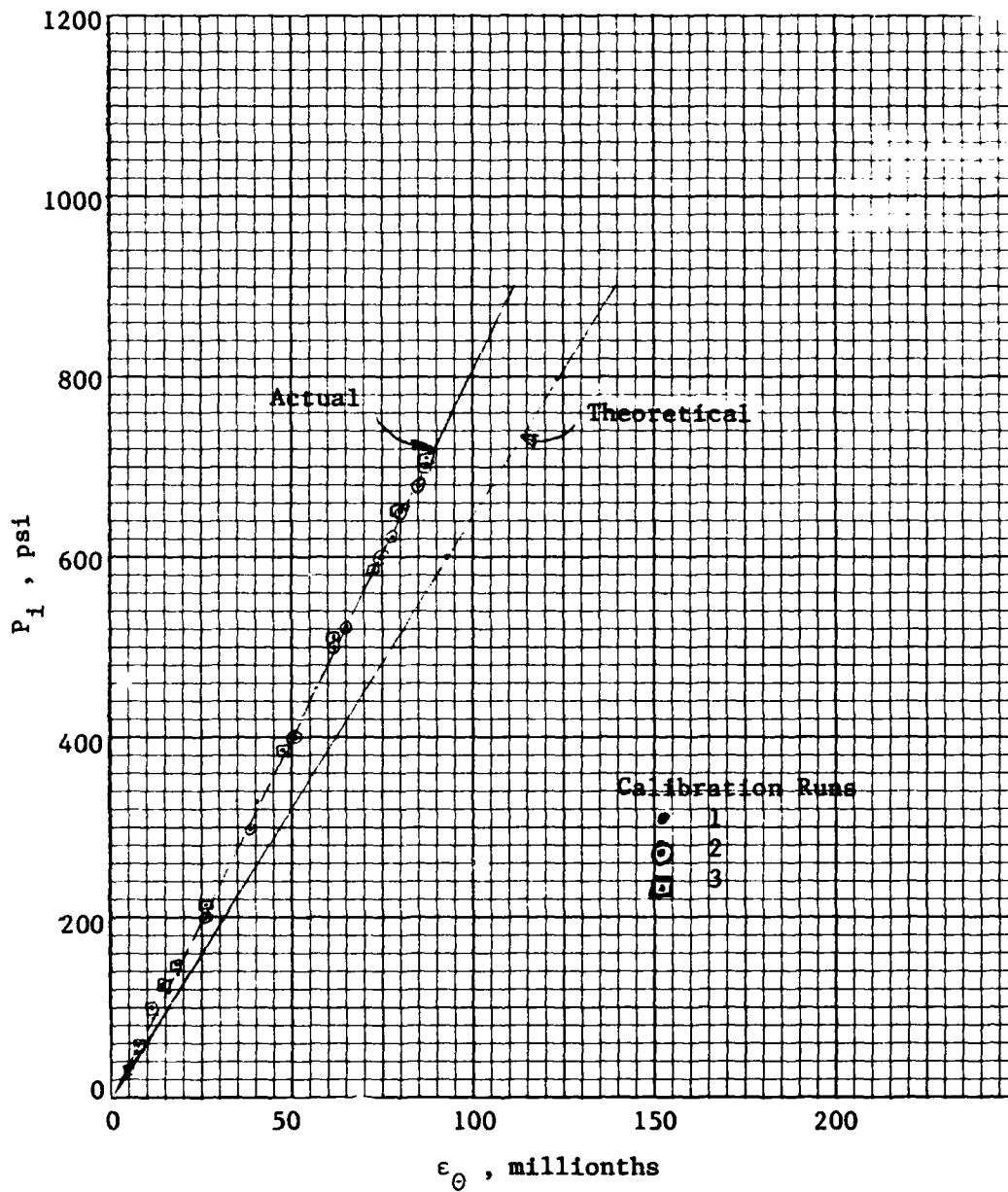


Figure 5. Theoretical and actual hoop strain on outside of grout cylinder mold; calibration tests

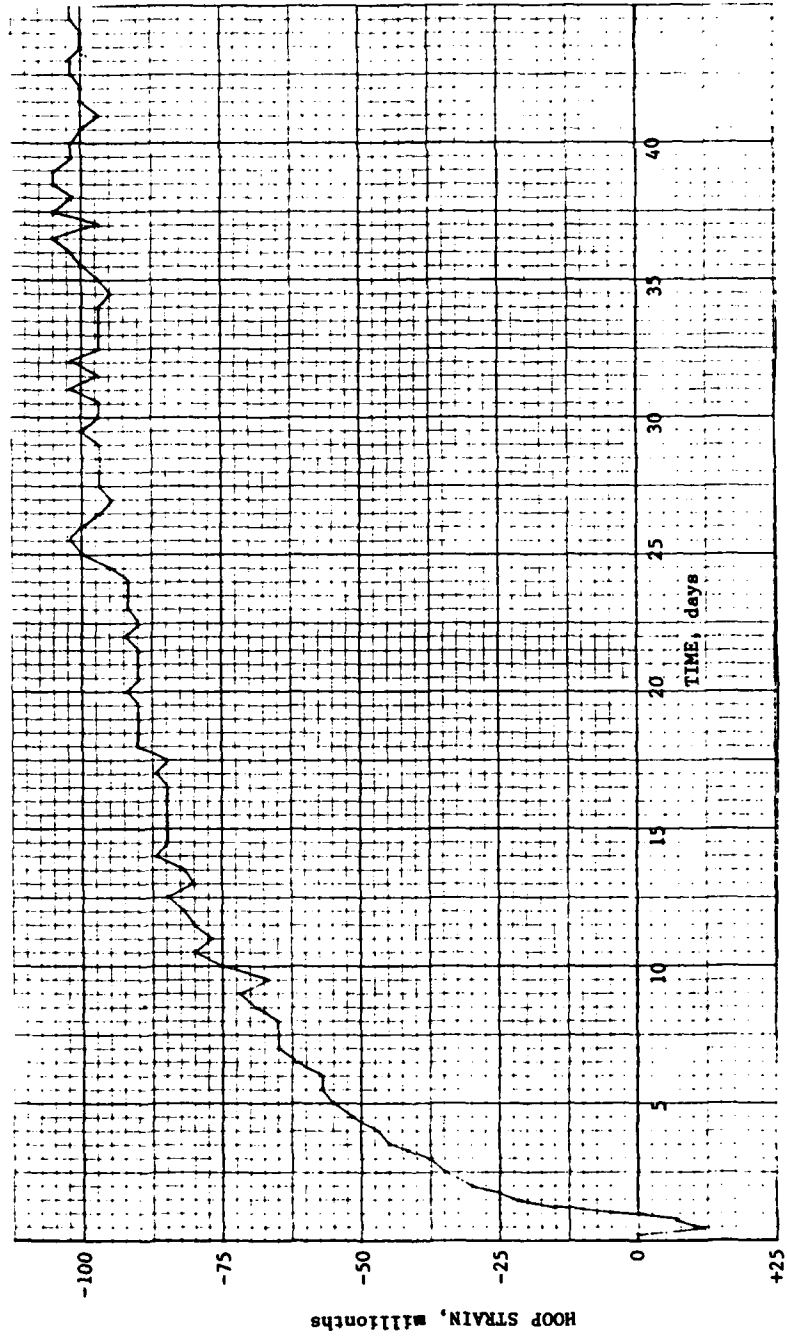


Figure 6. Hoop strain versus time for BCT-1-FF grout in cylinder mold

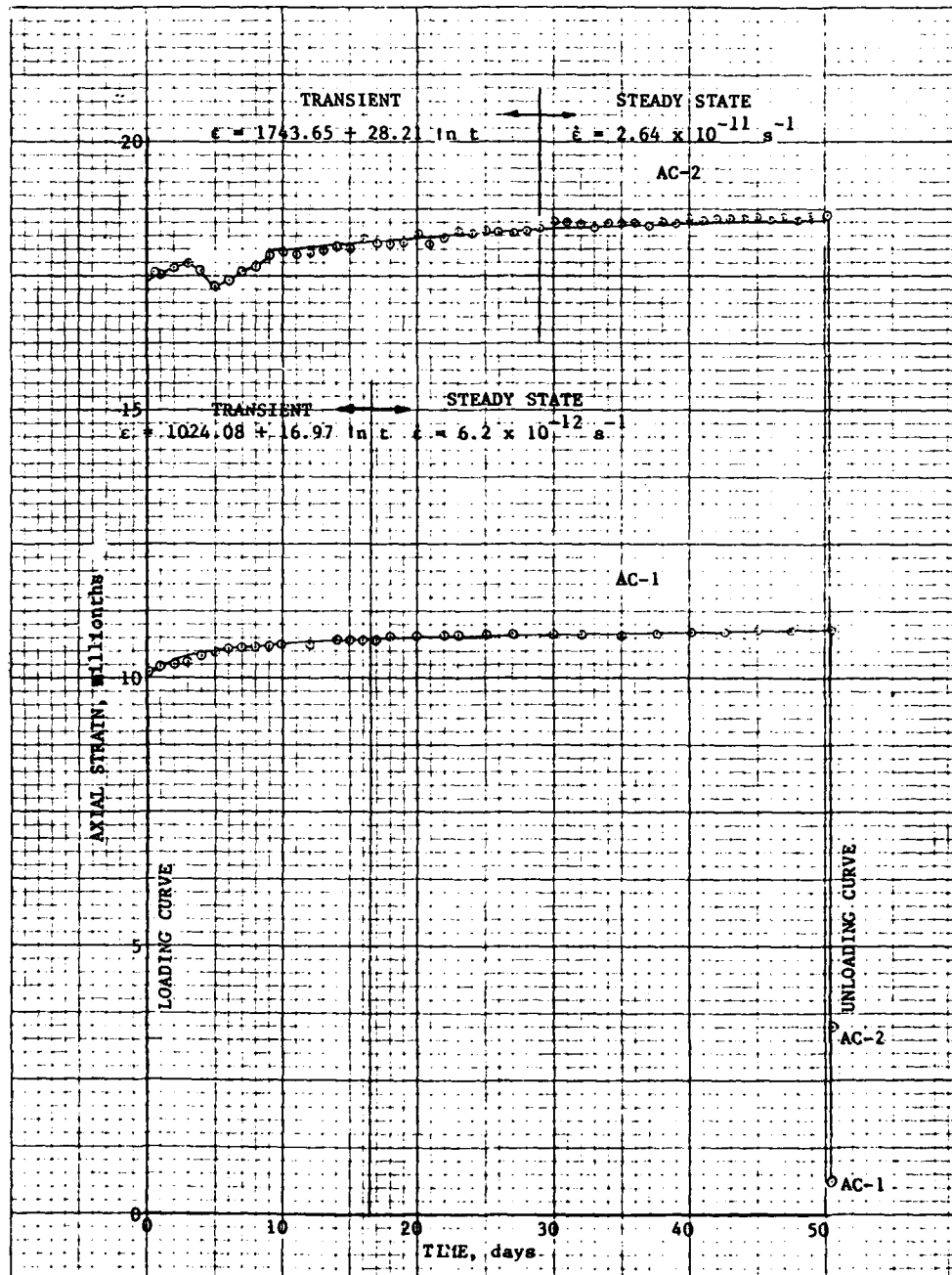


Figure 7. Axial creep curve as a function of time, anhydrite specimens AC-1 and AC-2



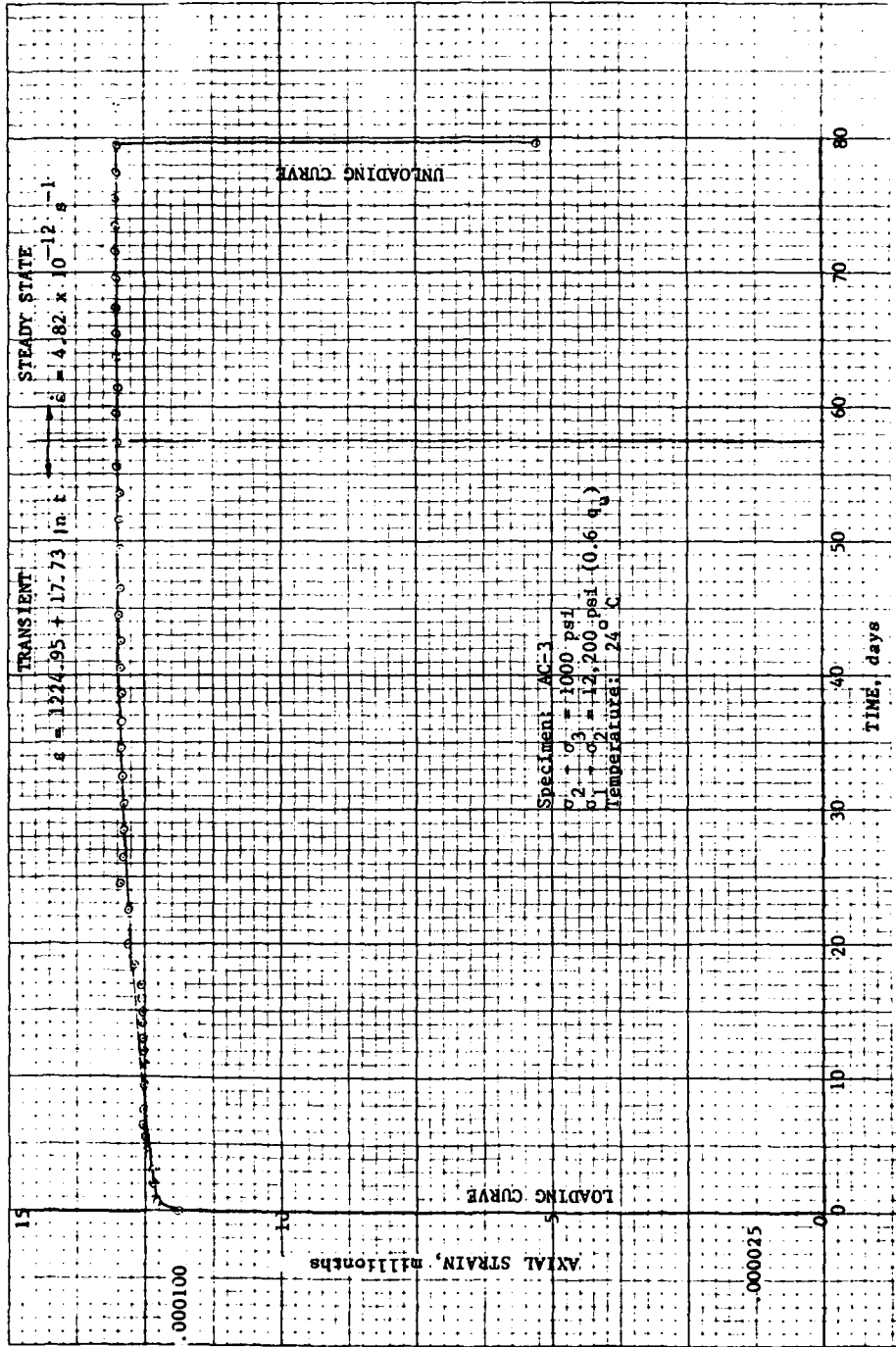


Figure 8. Axial creep curve as a function of time, anhydrite

**END**

**FILMED**

**12-85**

**DTIC**